Downscaled Climate Change Scenarios for Baja California and the North American Monsoon during the Twenty-First Century

TEREZA CAVAZOS AND SARAHÍ ARRIAGA-RAMÍREZ

Department of Physical Oceanography, Centro de Investigación Científica y de Educación Superior de Ensenada, Ensenada, Baja California, Mexico

(Manuscript received 9 August 2011, in final form 5 April 2012)

ABSTRACT

Regional climate change scenarios for Baja California/Southern California (BCC) and the North American monsoon (NAM) were produced as part of the Baja California State Climate Change Action Program (PEACC-BC). Bias-corrected and spatially downscaled scenarios (BCSD) from six general circulation models (GCMs) with a total of 12 realizations were analyzed for two scenarios of the Intergovernmental Panel on Climate Change (IPCC) Special Report on Emissions Scenarios (SRES): B1 (low emissions) and A2 (high emissions) during the twenty-first century. A validation of the original GCM realizations and the BCSD scenarios with observed data during 1961–90 show that the ensemble GCM produces too much precipitation during autumn and winter, which could be the cause of the observed delay of the summer monsoon rains; the ensemble BCSD considerably improves the mean annual cycles and spatial distributions of precipitation and temperature in the region. However, both ensembles greatly underestimate the observed interannual variability of precipitation. BCSD scenarios of temperature and precipitation during the twenty-first century were evaluated on the basis of the multimodel median change relative to 1961–90. The scenarios of precipitation change show large interannual variations and larger uncertainties than the scenarios of temperature change. The A2 scenarios show the largest reductions of precipitation in the last 20 yr of the twenty-first century; a decrease of 30% is projected for BCC mainly in winter and spring, while precipitation in the NAM region could be weakened by 20% during winter, spring, and summer. After 2050, a significant reduction of precipitation is expected in northwestern Mexico and the southwestern United States south of 35°N, and temperature changes larger than 2°C warming.

1. Introduction

The increased recognition that our climate is changing has produced a demand for climate change information at local and regional scales for use in integrated assessments of climate change on human and natural systems (e.g., Milly et al. 2008; Giorgi et al. 2009). The 2008–2013 Development Plan of the State of Baja California, Mexico, recognized the protection and sustainability of the environment as one of the transversal axes of development. In May 2008 the Ministry of Environmental Protection of the Government of Baja California invited three local academic institutions [Centro de Investigación Científica y de Educación Superior de Ensenada (CICESE), Universidad Autónoma de Baja California (UABC), and El Colegio de la Frontera Norte (COLEF)] to develop the State Climate Change Action Program of Baja California (PEACC-BC). One of the objectives of the PEACC-BC, and the aim of this article, is to evaluate downscaled climate change scenarios of temperature and precipitation not only for Baja California (BCC in Fig. 1a), but also for the North American monsoon (NAM) region and the southwestern United States (SW-U.S.) to assess the extension of the future changes of this semiarid region.

Northwestern Mexico (NW-Mex) and the SW-U.S. have already experienced significant increases of surface temperature during the last quarter of the twentieth century, likely associated with anthropogenic greenhouse gases (Karoly and Wu 2005), with further warming and drying likely to occur during the twenty-first century (e.g., Solomon et al. 2007; Seager et al. 2007; Christensen and Lettenmaier 2006; Montero-Martínez and Pérez-López 2008; Cayan et al. 2008; Diffenbaugh et al. 2008; Giorgi and Bi 2009; Conde et al. 2011).

Corresponding author address: Tereza Cavazos, Departamento de Oceanografía Física, CICESE-Ensenada, P.O. Box 434844, San Diego, CA 92143.
E-mail: tcavazos@cicese.mx

DOI: 10.1175/JCLI-D-11-00425.1

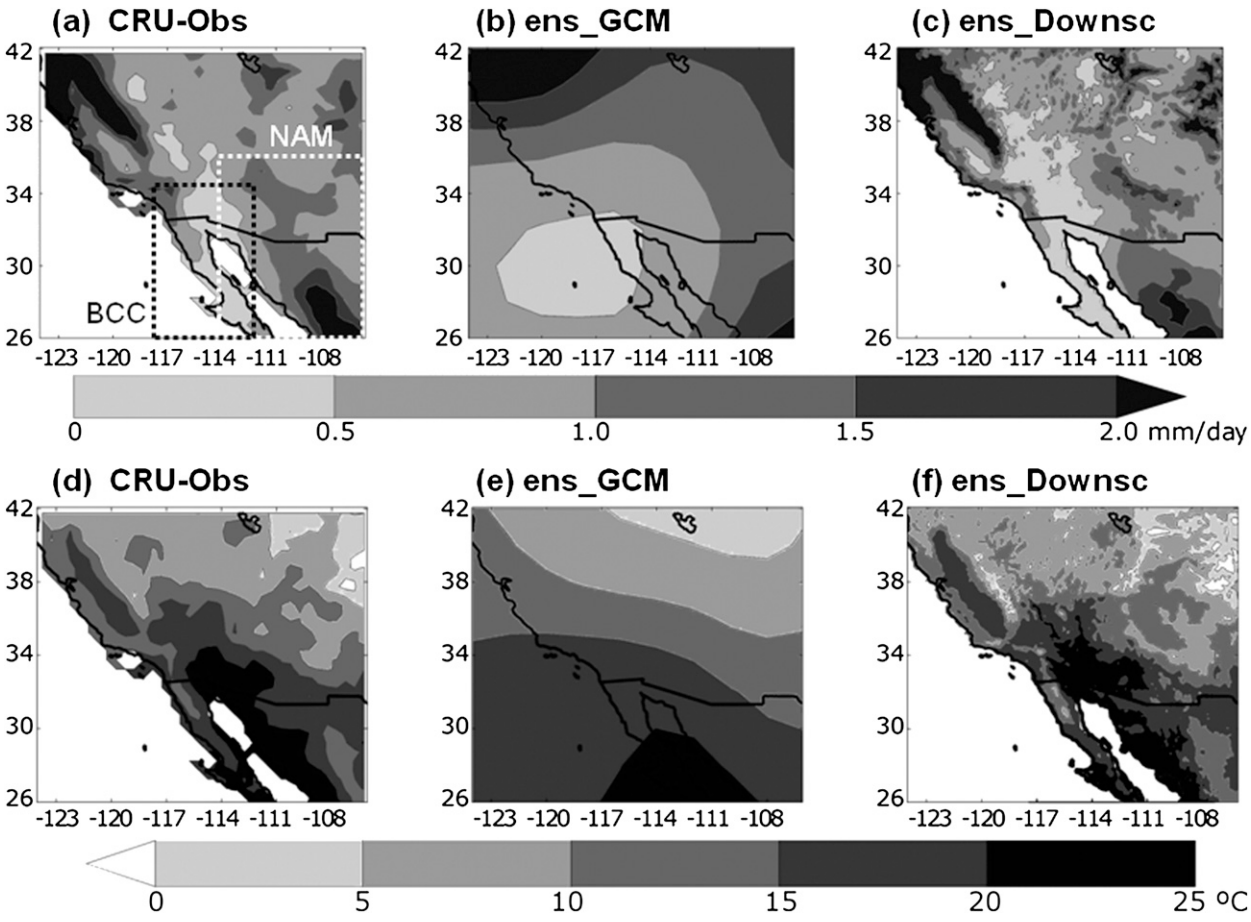

FIG. 1. Mean annual precipitation (mm day^{-1}) and mean annual temperature (°C) during 1961–90 for (a),(d) observed data from the CRU monthly gridded dataset (0.5° × 0.5° resolution), (b),(e) median ensemble of the GCM (2° × 2° resolution), and (c),(f) median ensemble of the BCSD ($^1/_8$° × $^1/_8$° resolution). Precipitation in the northwestern corner of (a)–(c) is not to scale (it goes up to 9 mm day^{-1}). The broken rectangles in (a) represent BCC and the NAM region.

The Fourth Assessment Report (AR4) of the Intergovernmental Panel on Climate Change (IPCC; Solomon et al. 2007) was based on 23 coupled ocean–atmosphere GCMs of the Coupled Model Intercomparison Project phase 3 (CMIP3) multimodel dataset. Several works have validated the GCMs of the CMIP3 dataset in different parts of the SW-U.S. and the NAM region (e.g., Giorgi and Bi 2005; Liang et al. 2006; Ruiz-Barradas and Nigam 2006; Brekke et al. 2008; Liang et al. 2008; Lin et al. 2008; Montero-Martínez and Pérez-López 2008; Arreola and Cavazos 2009; Gao et al. 2011). For example, Liang et al. (2008) and Lin et al. (2008) validated 22 GCMs using several metrics relevant to the intraseasonal and interannual variability of the NAM system. Lin et al. (2008) found that most of the GCMs reproduced the monsoon rainbelt and its gradual northward shift in early summer, but the majority overestimated the seasonal precipitation, especially in autumn and winter, consistent with Liang et al. (2008) and Arreola and Cavazos (2009), thus failing to reproduce the monsoon retreat in the fall. On the other hand, Kim et al. (2008) found that medium- and high-resolution GCMs of the CMIP3 dataset better reproduced the NAM precipitation pattern than those of low resolution (greater than ~3.75° × 3.75°).

Many studies have assessed either statistical or dynamical climate downscaling analyses to reduce GCM biases at regional scale. These studies agree on that 1) statistical downscaling offers a relatively quick and cheap method to generate useful information for decision making and integrated assessments but depends on the reliability of the large-scale driving predictors, season of the year, and topography (e.g., Cavazos and Hewitson 2005), and fails to capture the dynamics and nonstationary aspects of climate (e.g., Fowler et al. 2007); and 2) dynamical downscaling takes into account the physics and the nonstationarity of climate, but it is computationally expensive, and strongly depends on the

TABLE 1. Coupled ocean–atmosphere GCMs from the CMIP3 dataset used in the evaluation of downscaled climate change scenarios. Column 3 shows the number of model realizations analyzed for B1 and A2 emissions scenarios and, in parentheses, the spatial resolution of the global atmospheric grid.

Model	Modeling group	No. of runs (resolution)
Bjerknes Centre for Climate Research Bergen Climate Model, version 2 (BCCR-BCM2.0)	Bjerknes Centre for Climatic Research, Norway	1 (high: 1.875° × 1.875°)
Canadian Centre for Climate Modelling and Analysis (CCCma) Coupled GCM, version 3.1 (CGCM3.1)	Canadian Centre for Climate Modelling and Analysis	5 (medium: 2.8125° × ~2.8125°)
Centre National de Recherches Météorologiques model, version 3 (CNRM-CM3)	Centre National de Recherches Météorologiques, France	1 (medium: 2.8125° × ~2.8125°)
Commonwealth Scientific and Industrial Research Organisation, Mark version 3.0 (CSIRO Mk3.0)	CSIRO Atmospheric Research, Australia	1 (high: 1.875° × ~1.875°)
The third climate configuration of the Met Office Unified Model (UKMO HadCM3)	Hadley Centre for Climate Prediction and Research, United Kingdom	1 (medium: 3.75° × 2.5°)
Model for Interdisciplinary Research on Climate 3.2 (MIROC3.2)	Center for Climate System Research, Japan	3 (medium: 2.8125° × ~2.8125°)

GCM boundary forcing, the regional model's cumulus parameterizations, and horizontal resolution (e.g., Liang et al. 2006; Fowler et al. 2007; Lee et al. 2007; Chan and Misra 2011; Gao et al. 2011).

In the long run, the best representation of climate and its future evolution might be given by high-resolution dynamical climate models, especially during summer when convective processes dominate (e.g., Pan et al. 2001; Cavazos and Hewitson 2005; Liang et al. 2006; Lee et al. 2007). However, at present, statistical downscaling techniques still offer an alternate solution for the development of regional climate change scenarios, and may serve for future comparisons with dynamical downscaling analyses. This study is focused on the evaluation of statistically downscaled monthly climate change projections for Baja California/Southern California (BCC) and the NAM region (Fig. 1a) derived from a bias-corrected and spatially downscaled technique (BCSD; Maurer et al. 2007). Based on previous studies (Liang et al. 2008; Lin et al. 2008; Arreola and Cavazos 2009), 6 medium- to high-resolution GCMs were selected (out of 22) for their ''best'' performance to reproduce different features of the seasonal and interannual climate of the NAM region during the base period of 1961–90 (Table 1). Because of uncertainties in future greenhouse gas (GHG) forcings, two extreme scenarios of the IPCC Special Report on Emissions Scenarios (SRES) were chosen: the B1 (low emissions) and the A2 (high emissions). The current CO_2 emission is 380 ppm. The B1 scenario assumes a stabilization of 550 ppm at the end of the twenty-first century, and the A2 scenario considers stabilization at 850 ppm, if carbon mitigation measures are not taken by the governments (Cayan et al. 2008).

This paper is organized as follows. Data and methodology are described in section 2. Section 3 shows the results of the validation of the raw GCMs and the BCSD projections during 1961–90. Climate change scenarios based on the median ensemble of the BCSD GCMs during the twenty-first century are presented in section 4. Some impacts are discussed in section 5, and the conclusions of this study are in section 5.

2. Data and methodology

The Lawrence Livermore National Laboratory (LLNL), Reclamation, Santa Clara University in California, and Climate Central developed statistically downscaled monthly climate change projections derived from the CMIP3 multimodel dataset for North America, north of 25°N, using a BCSD technique described by Maurer et al. (2007). This dataset has been used in several hydrologic impact analyses of the western United States (e.g., Wood et al. 2004; Christensen and Lettenmaier 2006) and in some of the California climate change scenario assessments (e.g., Cayan et al. 2008). The downscaled archive was originally developed for monthly values of temperature and precipitation for several IPCC SRES emissions scenarios to provide planning analysts access to climate change projections downscaled to a finer resolution ($1/8° \cong 12$ km). At the time of the revision of this article, downscaled archives

were also available at daily time scale and for more variables. The archive with the downscaled multimodel dataset is freely available at http://gdo-dcp.ucllnl.org/downscaled_cmip3_projections/. Details of the BCSD technique are available in the same site. Apart from the typical advantages and disadvantages of a statistical downscaling method, described in the introduction, it is important to notice that 1) the BCSD technique is not based on the downscaling of large-scale atmospheric predictors, but on correcting GCM biases as compared to observations, and 2) the downscaled GCM biases have the same structure during the twentieth and twenty-first centuries. Wood et al. (2004) found that monthly bias-corrected data reproduced observed hydrology reasonably well in the western United States but failed to reproduce subtle differences between model and observed data; thus, a daily downscaling may be needed to reduce these biases. This technique has been successfully used to bias correct regional climate model output (e.g., Kleinn et al. 2005), but with less success at high elevations.

The BCSD projections of the B1 and A2 IPCC SRES emissions scenarios of the 6 GCMs and their member realizations (12 in total) used in this study are shown in Table 1. Liang et al. (2008) found that the Meteorological Research Institute of Japan (MRI) GCM was the GCM (out of 18 models) that best reproduced different features of the NAM system, but the BCSD output of this model was not available. For validation purposes, the raw GCM realizations were also obtained from the same site as the BCSD projections at a common grid (2.0° × 2.0° resolution). A validation of the raw GCMs and the BCSD projections during the base period (1961–90) was assessed with an independent observed dataset of temperature and precipitation than the one used to produce the BCSD projections (Maurer et al. 2007). The Climatic Research Unit (CRU) observed monthly gridded dataset (0.5° × 0.5° resolution) of the University of East Anglia (Mitchell and Jones 2005; dataset available online at http://www.cru.uea.ac.uk/cru/data/hrg/cru_ts_2.10/data_all/) was used for validation. The three datasets were regridded to a common 2° × 2° resolution to obtain annual cycles of mean temperature and precipitation and interannual errors [root-mean-square errors (RMSE) and mean absolute errors (MAE)] for the BCC and NAM regions; as an example, the validation results of the NAM region are shown in the following section.

After validation, the downscaled (BCSD) annual and seasonal (December–February, March–May, June–August, and September–November) differences, or changes, of the ensemble median fields of temperature and precipitation between two 20-yr periods of the twenty-first century (2010–29 and 2080–99) and the reference period 1961–90 were analyzed. Changes in each gridpoint were calculated in the following way: 1) individual annual anomaly fields for each of the 12 BCSD realizations relative to 1961–90; 2) median of the annual anomalies of the multimodel ensemble (annual median change in a gridpoint = A_{median}); 3) for the seasonal projections, the annual median changes were decomposed onto their seasonal changes; 4) for the bidecadal periods, A_{median} was averaged over the 20 yr $A_{\text{20-yr\_median}}$ and its sign was checked; and 5) 20-yr average of the annual anomalies of each realization $A_{\text{20-yr\_realizations}}$ were obtained; if ⅔ of the $A_{\text{20-yr\_realizations}}$ had the same sign as the $A_{\text{20-yr\_median}}$, then $A_{\text{20-yr\_median}}$ in the gridpoint was considered as significant, as done by the AR4 of the IPCC (Solomon et al. 2007).

For the time series of the annual change representative of a spatial window, the A_{median} was averaged over all grid points to obtain $\text{AA}_{\text{median}}$. To determine the annual uncertainty (or dispersion) representative of the same spatial window, the average median (over all grid points) of each model realization X_j was compared with the sign of $\text{AA}_{\text{median}}$. The uncertainty of the year i was calculated with the median absolute deviation (MAD) of all the $X_j(i)$ that had the same sign as the $\text{AA}_{\text{median}}$:

$$\text{MAD}_i = \text{median}_i[|X_j(i) - \text{AA}_{\text{median}}(i)|]. \quad (1)$$

The resultant annual MAD was plotted (±0.5 MAD) around the average median change in the time series of each year; this is indicated as the shaded areas of the time series. Furthermore, for the precipitation changes the sign of $\text{AA}_{\text{median}}$ in a particular year was considered as significant when ⅔ of the model realizations agreed on the sign of $\text{AA}_{\text{median}}$ (i.e., consensus) (see dots in Fig. 5).

3. Validation of the downscaled data during 1961–90

The winter climate of the entire region in Fig. 1 is particularly modulated by El Niño–Southern Oscillation (ENSO) at interannual time scales and the Pacific decadal oscillation (PDO; Mantua et al. 1997) at decadal time scales, with wetter (drier) winter conditions associated with El Niño/+PDO (La Niña/−PDO) phases (e.g., Gershunov and Barnett 1998; Pavia et al. 2006; Arriaga-Ramirez and Cavazos 2010). The NAM region (Fig. 1a) is characterized by a semiarid climate mainly influenced by the summer monsoon system, which is responsible for a large proportion (~65%) of the annual precipitation (Arriaga-Ramirez and Cavazos 2010). However, tropical cyclones during summer and early

autumn, as well as frontal systems and troughs within the subtropical westerly jet during winter, are also common in the region.

The state of Baja California is located in NW-Mex between 28° and 32°N in the driest part of the country, where annual precipitation is less than 300 mm ($<$1 mm day^{-1}), as seen in the BCC region in Figs. 1a,c. BCC has two major climatic regions: the northwestern corner is characterized by a semiarid Mediterranean climate with annual precipitation greater than 0.5 mm day^{-1}, and the eastern and southern part of BCC is a desert with less than 0.5 mm day^{-1}. The multimodel downscaled (BCSD) median ensemble (ens_Downsc) in Fig. 1 is able to capture very well the observed precipitation and temperature patterns of the entire region. In contrast, the multimodel ensemble GCM (ens_GCM) in Fig. 1b does not reproduce adequately the Mediterranean precipitation region nor the desert area of BCC; it does produce a meridional gradient of temperature (Fig. 1e) that it is also seen in the observations (CRU-Obs; Fig. 1d) and in the ens_Downsc (Fig. 1f) patterns. However, the ens_GCM fails to reproduce the extension of the desert area into Arizona ($T > 20$°C; $P <$ 0.5 mm day^{-1}) and some features related with topographic effects, as was expected because of the coarse resolution of the GCMs.

Figures 2 and 3 show the results of the validation of the raw GCMs and the BCSD projections compared to observed mean temperature and precipitation in the NAM region. The raw GCM realizations shown in Fig. 2a tend to overestimate precipitation during autumn, winter, and spring, and to underestimate rainfall during the peak of the monsoon in July and August. In general, the monsoon is delayed in the majority of the GCMs and these fail to produce the monsoon precipitation retreat at the end of summer. Similar patterns were observed with other GCMs not considered in this analysis (Wang et al. 2009), but with larger errors (e.g., Liang et al. 2008; Arreola and Cavazos 2009), or larger phase shifts in the annual cycle (e.g., Liang et al. 2008). The mean and median ensemble GCMs of the annual cycle of precipitation were very similar. Averaging individual realizations of the two GCMs that have several realizations, before the ensemble, produced a slightly larger overestimation of autumn rainfall than the one obtained with the median ensemble (ens_GCM) in Fig. 2a. The median BCSD ensemble (ens_Downsc) reproduces the annual cycle very well.

The large autumn and winter precipitation totals produced by some GCMs could be partially responsible for the delay of the onset of the summer monsoon rains (Fig. 2a), as has been found in observational studies of the NAM (e.g., Higgins et al. 1998; Hu and Song 2002; Zhu et al. 2005, 2007) and suggested by modeling studies (e.g., Seth et al. 2011). Moreover, a possible land surface effect of the overestimation of precipitation before the monsoon is the surface cooling effect seen in winter and spring in the ens_GCM of temperature in Fig. 2b. Observational studies have shown that this mechanism tends to delay the onset of the monsoon, but it varies on decadal time scales (e.g., Zhu et al. 2005, 2007).

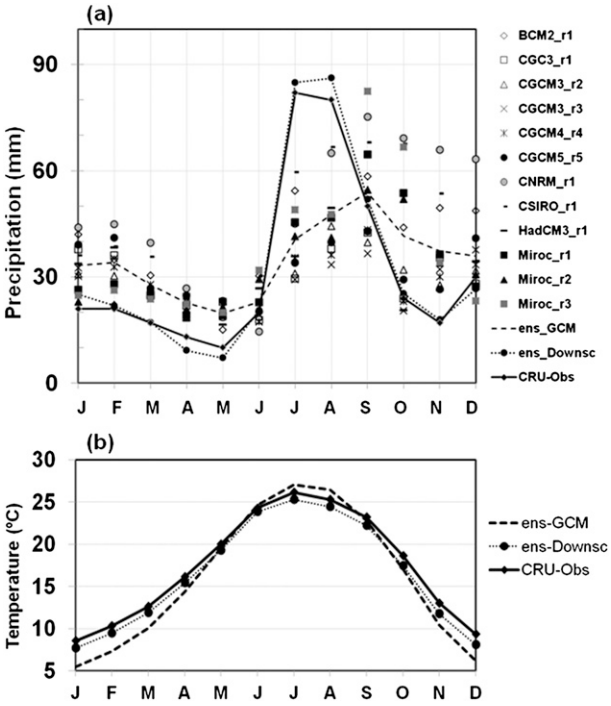

FIG. 2. Annual cycles of (a) precipitation (mm) and (b) temperature (°C) in the NAM region during 1961–90 as depicted by the raw GCMs in Table 1, its median ensemble (ens_GCM), the median BCSD ensemble (ens_Downsc), and observed data (CRU-Obs).

The BCSD technique partially corrects for the GCM biases of the annual cycles of precipitation and temperature, as seen in the ens_Downsc in Fig. 2. Obviously, this bias correction does not rectify the physical forcing mechanisms behind the wet and cool GCM biases, which may be associated with the GCMs' representation of the ENSO evolution (e.g., Guilyardi et al. 2009) and its teleconnections to the subtropics, as well as with other more complex mechanisms (e.g., Liang et al. 2006; Lee et al. 2007; Gao et al. 2011; Seth et al. 2011) that would need to be corrected by finer-resolution GCMs or regional climate dynamical models.

At interannual time scales, there are also large intermodel precipitation differences (Fig. 3a); the largest RMS and MAE errors (~0.6 mm day^{-1}) were obtained with Centre National de Recherches Météorologiques (CNRM) and Commonwealth Scientific and Industrial

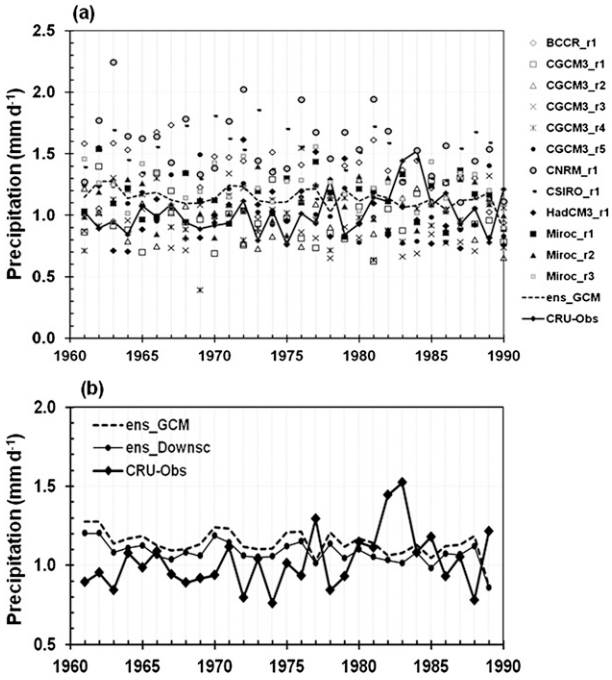

FIG. 3. As in Fig. 2, but for the interannual variations of precipitation (mm day^{-1}) in the NAM region.

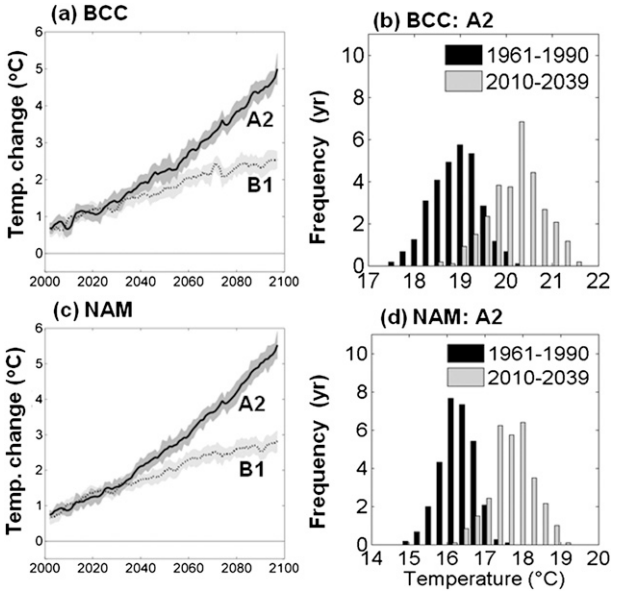

FIG. 4. (a),(c) Downscaled (BCSD) projections of the median change of annual temperature (°C) for BCC and the NAM region, respectively, from an ensemble of 6 GCMs with 12 realizations (Table 1) and under the B1 and A2 IPCC SRES emissions scenarios. Changes are relative to the 1961–90 base period means, and are filtered with a 5-yr weighted moving average (0.1, 0.2, 0.4, 0.2, and 0.1). Shading shows the annual uncertainty based on the median absolute deviation of all the realizations that had the same sign as the average median change in each individual year. (b),(d) Multimodel ensemble of the annual frequency distribution of temperature under the A2 scenario for 1961–90 and 2010–39.

Research Organisation (CSIRO); the other GCMs showed smaller precipitation errors, between 0.3 and 0.4 mm day^{-1}. Both multimodel ensembles (ens_GCM and ens_Downsc) tend to overestimate the mean annual precipitation (Fig. 3b) and underestimate the magnitude of the observed interannual precipitation variability. Thus, the advantage of the ens_Downsc projections over the ens_GCM is the more realistic spatial representation of the climatological precipitation and temperature patterns at regional scale (Figs. 1c,f) and the improvement of the mean annual cycles (Fig. 2).

4. Downscaled (BCSD) climate change scenarios during the twenty-first century

During the twenty-first century, BCC and the NAM region show positive trends in the median change of annual temperature with an increase of approximately 1.5°C by 2040, relative to 1961–90 under the high (A2) and low (B1) scenarios (Fig. 4). The frequency distributions in Fig. 4 show a positive displacement of the mean annual temperature in 2010–39, relative to 1961–90; the mean temperature in BCC is projected to increase from 19° to 20.5°C and, in the NAM region, from 16.3° to 17.8°C. After 2040 (Figs. 4a,c), the two scenarios steadily separate from each other, reaching an increase of approximately 3°C under the most optimistic B1 scenario and 5°C under the extreme A2 scenario. By the 2050s, a possible result of not taking global and regional mitigation measures (i.e., A2 scenario) begins to emerge. The multimodel ensemble shows a strong consistency in the median projections of temperature, as seen in the interannual uncertainty (shaded areas) in Figs. 4a,c.

In contrast to temperature, the projected changes of annual precipitation show larger uncertainties and larger interannual variability in BCC and the NAM region, but with a significant long-term negative trend in the A2 emissions scenario (Fig. 5). The most extreme scenario, and the strongest consensus among the models, is seen under A2, which shows an average decrease of 30% ± 5% of precipitation in the second half of the twenty-first century in BCC and an average reduction of 20% ± 5% of precipitation in the NAM region, relative to 1961–90 (Figs. 5b,d). The precipitation projected by the B1 scenario is approximately half of the one projected by A2 (Figs. 5a,c).

The spatial changes of precipitation in two 20-yr periods of the twenty-first century (2010–29 and 2080–99) suggest that the Mexico–U.S. western border region may become a hotspot under extreme (A2 scenario) warming conditions (Fig. 4) and reduced precipitation

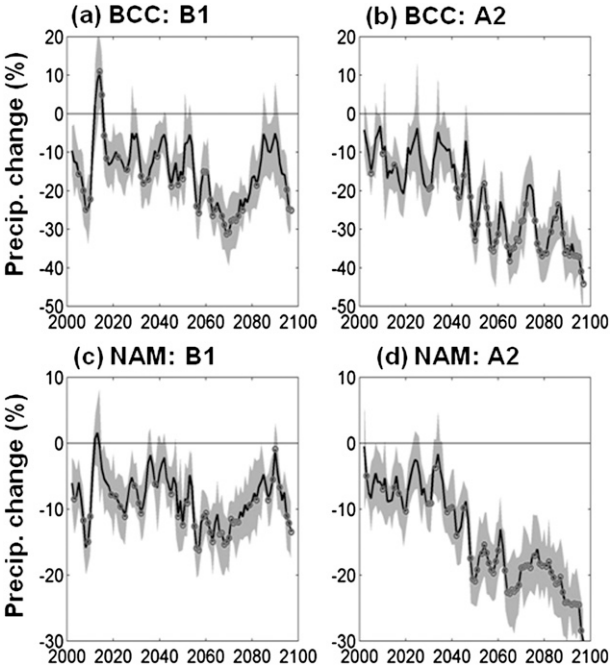

FIG. 5. As in Figs. 4a,c, but for the annual precipitation changes (%). Dots represent the years in which 2/3 of the realizations coincided on the sign of the average median change of precipitation (significant agreement).

(Figs. 5 and 6), especially at the end of the century. The Mexico–U.S. western border region has been already identified as a possible hotspot under climate change (Diffenbaugh et al. 2008; Giorgi and Bi 2009). North of 36°N, large areas of the SW-U.S. show large uncertainties in the scenarios of annual precipitation change (white areas in Fig. 6), possibly because this is the transition zone of the subtropical Pacific westerly jet stream (the northern branch of the Hadley cell), which is expected to migrate poleward under warming conditions (Lu et al. 2007), as well as the position of the storm tracks (e.g., Yin 2005; Solomon et al. 2007; Favre and Gershunov 2008). Accordingly, small positive precipitation changes (~5%–10%) are projected for the northern boundary of the study area (~40°N) in the upper Colorado River basin at the end of the twenty-first century (Fig. 6) and during winter (Fig. 7a).

At seasonal time scales, the strongest drying scenarios in the Mexico–U.S. western border region under both B1 (not shown) and A2 emission scenarios are expected to occur in BCC in winter and spring of 2080–99 (Figs. 7 and 8b), which is in agreement with Giorgi and Bi (2009). Small positive precipitation changes (~5%) are projected for summer in the coastal Mediterranean region of Baja California and California (Fig. 7c). Autumn is the season that showed the smallest changes in the entire region and during the entire period.

The largest decreases of precipitation in the NAM region are also expected to occur in the second half of the twenty-first century (Fig. 5d) in winter and summer in the core monsoon region in NW-Mex (Fig. 7) and in winter and spring in the northern part of the monsoon region (i.e., Arizona, the lower Colorado River basin, and New Mexico), as seen in the seasonal changes in Figs. 7 and 8.

5. Discussion of impacts

Arid and semiarid regions of northern Mexico and the SW-U.S. are particularly vulnerable to the impacts of climate change. The results show that mean annual temperature may increase 1.5°C in the next 30 yr and approximately 5°C at the end of the twenty-first century under the A2 scenario. Even the most optimistic B1 scenario projects temperature changes larger than the 2°C warming target set to avoid dangerous climate change by the 2010 United Nations Cancun Agreement (AWGLCA 2010). Arora et al. (2011), using a new set of GHG scenarios, suggest that limiting global warming to 2°C by the end of this century is unlikely since it requires immediate action.

Winter and spring precipitation in BCC is expected to decrease 15% in the next 30 yr and about 30% by the end of the century under the A2 scenario. However, small positive precipitation changes (~5%) are projected for the summer-dry season of Baja California and California, possibly associated with a stronger land–sea thermal contrast (e.g., Sutton et al. 2007; Snyder et al. 2003) and stronger upwelling along the California Current during the summer months (Snyder et al. 2003), as has been suggested to occur under global warming.

Warmer conditions may affect different sectors of BCC; for example, the viniculture—wine production in Baja California accounts for 85% of the total national production (Trejo-Pech et al. 2012). According to Jones (2007), average temperatures between 13° and 24°C during the growing season (April–October) are required (among other factors) for high- to premium-quality wine production in the world's benchmark regions. The upper temperature limit for grape production lies between 19° and 24°C; based on this temperature range (see, e.g., Fig. 8a), by the end of this century the grape production in Baja California could be reduced to 4 varietals (out of 10 currently produced; Trejo-Pech et al. 2012)—that is, cabernet sauvignon, grenache, zinfandel, and nebbiolo, which are the most tolerant grapes to warmer conditions (Jones 2007). However, local wine makers consider that the most damaging factors for grape and wine productions are extreme events, such as too-wet

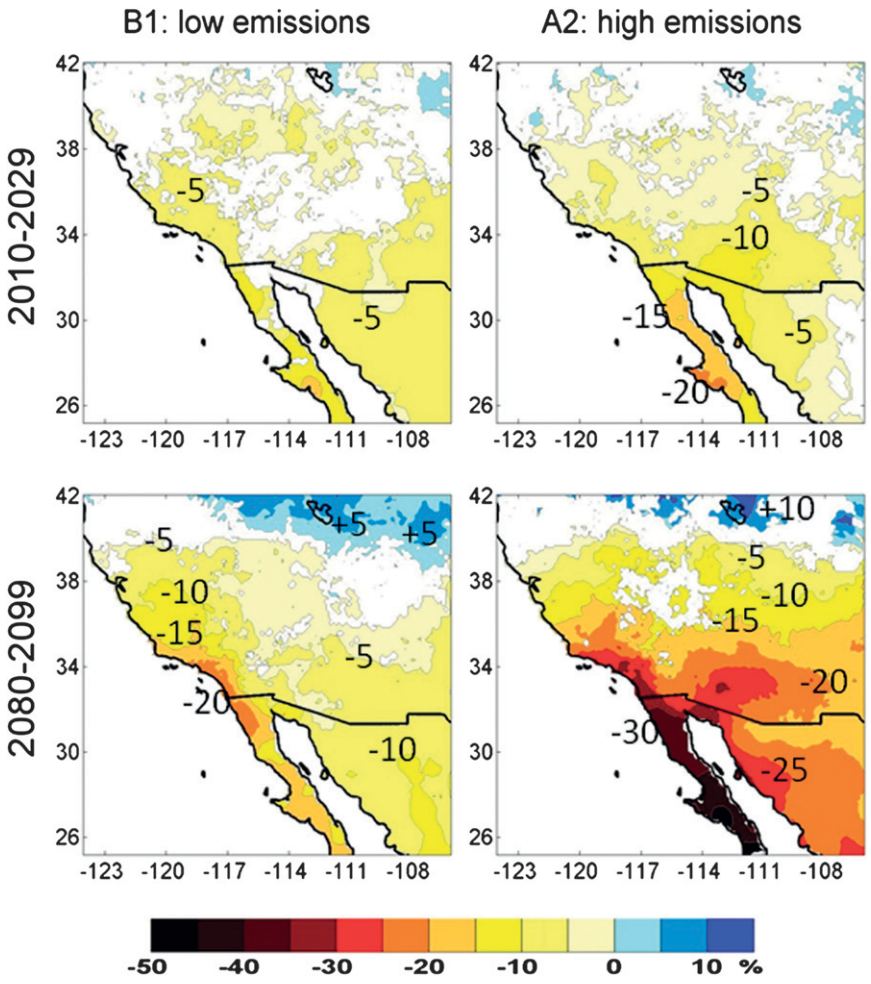

FIG. 6. Downscaled spatial projections of the median change of precipitation (%) for two 20-yr periods and two emissions scenarios from the ensemble of the 6 GCMs with 12 realizations. Color-shaded regions indicate that 2/3 of the model realizations agree on the sign of change (significant agreement). White areas indicate that there is not a significant agreement on the sign of change. Changes are relative to the 1961–90 base period means.

conditions, intense heat waves, summer rains, and droughts (water availability).

Water is the lifeblood of NW-Mex and it is also the limiting factor for its development; the agriculture sector alone uses 78% of the available water and, if population continues to grow as the future scenarios indicate, the region may become very vulnerable because of water scarcity (CONAGUA 2008) and water conflicts between sectors, and even conflicts at a binational level. For example, 50% of the surface water in Baja California comes from the Colorado River water allocations to Mexico, which are mainly used by the agricultural sector from Mexicali to Tijuana along the western Mexico–U.S. border. The drying trend found in this study is consistent with hydrologic analyses in the SW-U.S. that show a dramatic decrease of runoff by the 2050s (Milly et al. 2008) and by the end of the twenty-first century in the Colorado River basin (Christensen et al. 2004; Christensen and Lettenmaier 2006), possibly associated with changes in snow cover and the timing of peak snowmelt in the mountains of the SW-U.S. due to increased warming. Christensen and Lettenmaier (2006) and Milly et al. (2008) suggest that surface water delivered to Mexico could be reduced by 10%–15% by 2050, thus providing new stresses on the existing water resources management structures in the Mexico–U.S. western border region (Das et al. 2009) and in BCC in coming decades.

The projected drying of the entire region south of 36°N—especially in winter, spring, and summer (Figs. 5 and 6)—has been attributed to global circulation changes associated with the poleward expansion of the subtropical

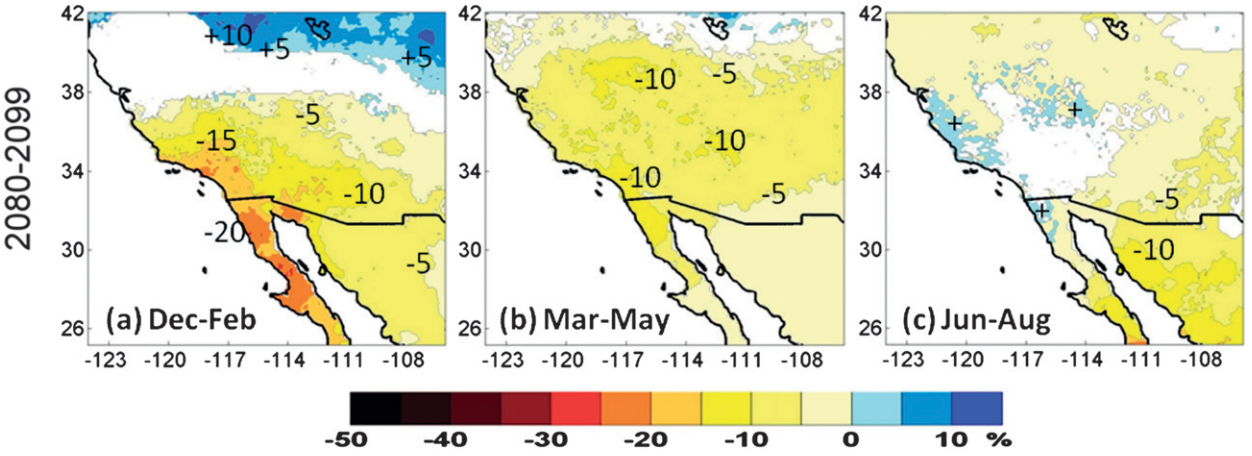

FIG. 7. Similar to Fig. 6, but for the seasonal precipitation changes [(a) December–February, (b) March–May, and (c) June–August] for 2080–99 under the A2 (high) emissions scenario. Some contours are shown for reference. Positive signs in (c) indicate values between 0% and 5% increases.

dry regions of the world (Seager et al. 2007) and a weakening of the Hadley circulation (e.g., Tanaka et al. 2005; Lu et al. 2007; Vecchi and Soden 2007) due to increased greenhouse gas emissions.

Tanaka et al. (2005), in a study of the response of the tropical circulation to increased GHG forcing, found a weakening not only of the Hadley circulation, but also of the Walker and global monsoon circulations at the end of the twenty-first century in most of the CMIP3 GCMs. The NAM system circulation is small compared to that of the Asian monsoon, but its regional impact has very important implications for society and for the semiarid environment, especially that the annual cycle of monsoon precipitation in the NAM region is expected to weaken by about 20% during the second half of the twenty-first century (Fig. 4d) under A2. However, precipitation in the region is also associated to natural variations, as mentioned in the introduction. Favre and Gershunov (2008) argue that interannual (ENSO) and decadal (PDO) variability in the study area will sometimes mask and sometimes intensify certain aspects of the projected regional changes over the coming decades. Partially consistent to Favre and Gershunov (2008), Dominguez et al. (2010) found that during the twenty-first century higher temperatures and lower precipitation in the upper part of the NAM region could be amplified during winters of La Niña.

6. Summary and conclusions

This study is focused on the evaluation of statistically downscaled monthly climate change projections for Baja California/Southern California (BCC) and the NAM region (Fig. 1a) derived from a bias-corrected and spatially downscaled technique. The validation results show that the ens_Downsc projections produce a more realistic spatial representation of precipitation and temperature at the regional scale (Figs. 1c,f) as well as a better representation of the mean annual cycles of temperature and precipitation than the ens_GCM (Fig. 2). However, both multimodel ensembles (ens_GCM and ens_Downsc) tend to overestimate the mean annual precipitation (Fig. 3b) and underestimate the magnitude of the observed interannual precipitation variability. This problem could be possibly reduced by using other types of downscaling methodologies, such as those based on atmospheric transfer functions (neural networks, multiple regression, etc.) or regional dynamical climate models.

Most of the raw GCMs show large positive (negative) biases in autumn and winter precipitation (temperature), which could be causing the delay of the summer monsoon rains during the observational period; thus, it will be important to see if the new CMIP phase 5 (CMIP5; Taylor et al. 2009) GCMs are able to reduce some of these biases.

All of the BCSD temperature scenarios of the twenty-first century showed a consensus on the sign of change (i.e., positive change), which is in contrast to the precipitation scenarios that showed large intermodel differences, which is consistent with the results of the AR4 of the IPCC (Solomon et al. 2007). The A2 scenarios show the largest reductions of precipitation in the last 20 yr of the twenty-first century; a decrease of 30% is projected for BCC mainly in winter and spring, while precipitation in the NAM region could be weakened by 20% during winter, spring, and summer. After 2050, a significant reduction of precipitation is expected in

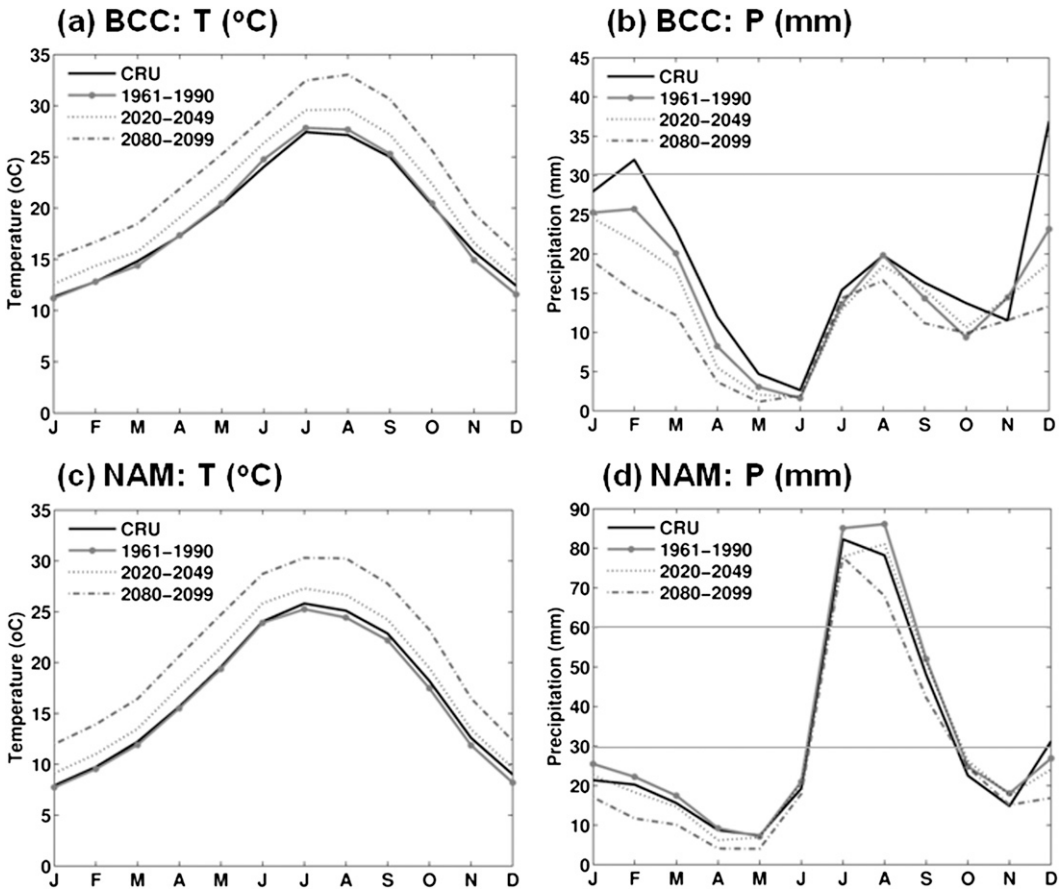

FIG. 8. Annual cycle of (left) temperature and (right) precipitation in (a),(b) BCC and (c),(d) the NAM region during different periods. CRU is the observed data during the reference period of 1961–90, and the other curves correspond to the multimodel ensemble (ens_Downsc) projections.

NW-Mex and the SW-U.S. south of 35°N and temperature changes larger than 2°C of warming.

The authors are currently analyzing the CMIP5 GCM projections to determine the dynamic and thermodynamic changes of the monsoon circulation in the NAM system in response to the projected global warming and land–sea thermal contrast. New downscaling initiatives both dynamical, like CORDEX (Giorgi et al. 2009), and statistical that may include the semiarid regions of BCC and the NAM will be very much welcome. These initiatives would favor a rapid dispersion of climate change downscaled scenarios for use in impact and adaptation studies, such as the PEACC-BC. The evaluation of the downscaled scenarios shown here are relevant for planning and adaptation strategies of the PEACC-BC and for understanding the Variability of American Monsoons (VAMOS) under global warming (e.g., Cavazos and Marengo 2008).

Acknowledgments. We appreciate the discussions with members of the PEACC-BC and with Sasha Gershunov, and the comments and suggestions of three anonymous reviewers. Partial funding for this work was provided by UC-Mexus-CONACYT, the Government of Baja California through the PEACC-BC, and a SEMARNAT-CONACYT project (2008–2012). We acknowledge the modeling groups, the Program for Climate Model Diagnosis and Intercomparison (PCMDI), and the WCRP's Working Group on Coupled Modelling (WGCM) for their roles in making available the WCRP CMIP3 multimodel dataset. The CMIP Data Archive at Lawrence Livermore National Laboratory is supported by the Office of Science, U.S. Department of Energy.

REFERENCES

Arora, V. K., and Coauthors, 2011: Carbon emission limits required to satisfy future representative concentration pathways of greenhouse gases. *Geophys. Res. Lett.,* **38,** L05805, doi:10.1029/2010GL046270.

Arreola, J. L., and T. Cavazos, 2009: Análisis de métricas climáticas para la evaluación de los modelos del IPCC en el noroeste de México y el suroeste de Estados Unidos. CICESE

Departamento de Oceanografia Fisica Comunicaciones Académicas, 13 pp.

Arriaga-Ramirez, S., and T. Cavazos, 2010: Regional trends of daily precipitation indices in northwest Mexico and southwest United States. *J. Geophys. Res.,* **115,** D14111, doi:10.1029/2009JD013248.

AWGLCA, 2010: Enhanced action on adaptation. Framework convention on climate change, UNFCCC revision of FCCC/AWGLCA/2010/14, 31–36.

Brekke, L. D., M. D. Dettinger, E. P. Maurer, and M. Anderson, 2008: Significance of model credibility in estimating climate projection distributions for regional hydroclimatological risk assessments. *Climatic Change,* **89,** 371–394, doi:10.1007/s10584-007-9388-3.

Cavazos, T., and B. C. Hewitson, 2005: Performance of NCEP–NCAR reanalysis variables in statistical downscaling of daily precipitation. *Climate Res.,* **28,** 95–107.

——, and J. A. Marengo, 2008: Activities on anthropogenic climate change. *CLIVAR Exchanges,* No. 48, International CLIVAR Project Office, Southampton, United Kingdom, 16–19.

Cayan, D. R., E. P. Maurer, M. D. Dettinger, M. Tyree, and K. Hayhoe, 2008: Climate change scenarios for the California region. *Climatic Change,* **87,** 21–42, doi:10.1007/s10584-007-9377-6.

Chan, S. C., and V. Misra, 2011: Dynamic downscaling of the North American monsoon with the NCEP–Scripps Regional Spectral Model from the NCEP CFS global model. *J. Climate,* **24,** 653–673.

Christensen, N. S., and D. P. Lettenmaier, 2006: A multimodel ensemble approach to assessment of climate change impacts on the hydrology and water resources of the Colorado River basin. *Hydrol. Earth Syst. Sci. Discuss.,* **3,** 1–44.

——, A. Wood, N. Voisin, D. P. Lettenmaier, and R. N. Palmer, 2004: The effects of climate change on the hydrology and water resources of the Colorado River basin. *Climatic Change,* **62,** 337–363.

CONAGUA, 2008: *Statistics on Water in Mexico*. SEMARNAT, 277 pp.

Conde, C., F. Estrada, B. Martinez, O. Sanchez, and C. Gay, 2011: Regional climate change scenarios for Mexico. *Atmósfera,* **24,** 125–140.

Das, T., and Coauthors, 2009: Structure and detectability of trends in hydrological measures over the western United States. *J. Hydrometeor.,* **10,** 871–892.

Diffenbaugh, N. S., F. Giorgi, and J. S. Pal, 2008: Climate change hotspots in the United States. *Geophys. Res. Lett.,* **35,** L16709, doi:10.1029/2008GL035075.

Dominguez, F., J. Cañon, and J. Valdes, 2010: IPCC-AR4 climate simulations for the southwestern US: The importance of future ENSO projections. *Climatic Change,* **99,** 499–514.

Favre, A., and A. Gershunov, 2008: North Pacific cyclonic and anticyclonic transients in a global warming context: Possible consequences for Western North American daily precipitation and temperature extremes. *Climate Dyn.,* **32,** 969–987, doi:10.1007/s00382-008-0417-3.

Fowler, H. J., S. Blenkinsop, and C. Tebaldi, 2007: Linking climate change modelling to impacts studies: Recent advances in downscaling techniques for hydrological modeling. *Int. J. Climatol.,* **27,** 1547–1578.

Gao, Y., J. A. Vano, C. Zhu, and D. P. Lettenmaier, 2011: Evaluating climate change over the Colorado River basin using regional climate models. *J. Geophys. Res.,* **116,** D13104, doi:10.1029/2010JD015278.

Gershunov, A., and T. Barnett, 1998: Interdecadal modulation of ENSO teleconnections. *Bull. Amer. Meteor. Soc.,* **79,** 2715–2725.

Giorgi, F., and X. Bi, 2005: Updates precipitation and temperature changes for the 21st century from ensembles of recent AOGCM simulations. *Geophys. Res. Lett.,* **32,** L21715, doi:10.1029/2005GL024288.

——, and ——, 2009: Time of emergence (TOE) of GHG-forced precipitation change hot-spots. *Geophys. Res. Lett.,* **36,** L06709, doi:10.1029/2009GL037593.

——, C. Jones, and G. R. Asrar, 2009: Addressing climate information needs at the regional level: The CORDEX framework. *WMO Bull.,* **58,** 175–183.

Guilyardi, E., A. Wittenberg, A. Fedorov, M. Collins, C. Wang, A. Capotondi, G. J. van Oldenborgh, and T. Stockdale, 2009: Understanding El Niño in ocean–atmosphere general circulation models: Progress and challenges. *Bull. Amer. Meteor. Soc.,* **90,** 325–340.

Higgins, R. W., K. C. Mo, and Y. Yao, 1998: Interannual variability of the U.S. summer precipitation regime with emphasis on the southwestern monsoon. *J. Climate,* **11,** 2582–2606.

Hu, Q., and F. Song, 2002: Interannual rainfall variations in the North American summer monsoon region: 1900–98. *J. Climate,* **15,** 1189–1202.

Jones, G. V., 2007: Climate change and the global wine industry. *Proc. 13th Australian Wine Industry Technical Conf.,* Adelaide, SA, Australia, AWITC, 91–98.

Karoly, D. J., and Q. Wu, 2005: Detection of regional surface temperature trends. *J. Climate,* **18,** 4337–4343.

Kim, H.-J., B. Wang, and Q. Ding, 2008: The global monsoon variability simulated by CMIP3 coupled climate models. *J. Climate,* **21,** 5271–5294.

Kleinn, J., C. Frei, J. Gurtz, D. Lüthi, P. L. Vidale, and C. Schär, 2005: Hydrologic simulations in the Rhine basin driven by a regional climate model. *J. Geophys. Res.,* **110,** D04102, doi:10.1029/2004JD005143.

Lee, M., and Coauthors, 2007: Sensitivity to horizontal resolution in the AGCM simulations of warm season diurnal cycle of precipitation over the United States and northern Mexico. *J. Climate,* **20,** 1862–1881.

Liang, X.-Z., J. Pan, J. Zhu, K. E. Kunkel, J. X. L. Wang, and A. Dai, 2006: Regional climate model downscaling of the U.S. summer climate and future change. *J. Geophys. Res.,* **111,** D10108, doi:10.1029/2005JD006685.

——, J. Zhu, K. E. Kunkel, M. Ting, and J. X. L. Wang, 2008: Do CGCMs simulate the North American monsoon precipitation seasonal–interannual variations. *J. Climate,* **21,** 4424–4448.

Lin, J. L., B. E. Mapes, K. M. Weickmann, G. N. Kiladis, S. D. Schubert, M. J. Suarez, J. T. Bacmeister, and M.-I. Lee, 2008: North American monsoon and associated intraseasonal variability simulated by IPCC AR4 coupled GCMs. *J. Climate,* **21,** 2919–2937.

Lu, J., G. A. Vecchi, and T. Reichler, 2007: Expansion of the Hadley cell under global warming. *Geophys. Res. Lett.,* **34,** L06805, doi:10.1029/2006GL028443.

Mantua, N. J., S. R. Hare, Y. Zhang, J. M. Wallace, and R. C. Francis, 1997: A Pacific interdecadal climate oscillation with impacts on salmon production. *Bull. Amer. Meteor. Soc.,* **78,** 1069–1079.

Maurer, E. P., L. Brekke, T. Pruitt, and P. B. Duffy, 2007: Fine-resolution climate projections enhance regional climate change impact studies. *Eos, Trans. Amer. Geophys. Union,* **88,** 504, doi:10.1029/2007EO470006.

Milly, P. C. D., J. Betancourt, M. Falkenmark, R. M. Hirsch, Z. W. Kundzewicz, D. P. Lettenmaier, and R. J. Stouffer, 2008: Stationarity is dead: Whither water management? *Science,* **319,** 573–574.

Mitchell, T. D., and P. D. Jones, 2005: An improved method of constructing a database of monthly climate observations and associated high-resolution grids. *Int. J. Climatol.,* **25,** 693–712.

Montero-Martínez, M., and J. L. Pérez-López, 2008: Regionalización de proyecciones climáticas en México de precipitación y temperatura en superficie usando el método REA para el siglo XXI. *Efectos del Cambio Climático en los Recursos Hídricos de México,* P. F. Martínez and A. Aguilar, Eds., Vol. 2, IMTA, 11–21.

Pan, Z., J. H. Christensen, R. W. Arrit, W. J. Gutowski Jr., E. S. Takle, and F. Otieno, 2001: Evaluation of uncertainties in regional climate change simulations. *J. Geophys. Res.,* **106** (D16), 17 735–17 751.

Pavia, E. G., F. Graef, and J. Reyes, 2006: PDO–ENSO effects in the climate of Mexico. *J. Climate,* **19,** 6433–6438.

Ruiz-Barradas, A., and S. Nigam, 2006: IPCC's twentieth-century climate simulations: Varied representations of North American hydroclimate variability. *J. Climate,* **19,** 4041–4058.

Seager, R., and Coauthors, 2007: Model projections of an imminent transition to a more arid climate in southwestern North America. *Science,* **316,** 1181–1184.

Seth, A., S. A. Rauscher, M. Rojas, A. Giannini, and S. J. Camargo, 2011: Enhanced spring convective barrier for monsoons in a warmer world? *Climatic Change,* **104,** 403–414, doi:10.1007/s10584-010-9973-8.

Snyder, M. A., L. C. Sloan, N. S. Diffenbaugh, and J. L. Bell, 2003: Future climate change and upwelling in the California Current. *Geophys. Res. Lett.,* **30,** 1823, doi:10.1029/2003GL017647.

Solomon, S., D. Qin, M. Manning, M. Marquis, K. Averyt, M. M. B. Tignor, H. L. Miller Jr., and Z. Chen, Eds., 2007: *Climate Change 2007: The Physical Science Basis*. Cambridge University Press, 996 pp.

Sutton, R. T., B. Dong, and J. M. Gregory, 2007: Land/sea warming ratio in response to climate change: IPCC AR4 model results and comparison with observations. *Geophys. Res. Lett.,* **34,** L02701, doi:10.1029/2006GL028164.

Tanaka, H. L., N. Ishizaki, and D. Nohara, 2005: Intercomparison of the intensities and trends of Hadley, Walker and monsoon circulations in the global warming projections. *SOLA,* **1,** 77–80.

Taylor, K. E., R. J. Stouffer, and G. E. Meehl, 2009: A summary of the CMIP5 experiment design. World Climate Research Programme Tech. Rep., 33 pp. [Available online at http://cmip-pcmdi.llnl.gov/cmip5/docs/Taylor_CMIP5_design.pdf.]

Trejo-Pech, C. O., R. Arellano-Sada, A. M. Coelho, and R. N. Weldon, 2012: Is the Baja California, Mexico, wine industry a cluster? *Amer. J. Agric. Econ.,* **94,** 569–575.

Vecchi, G. A., and B. J. Soden, 2007: Global warming and the weakening of the tropical circulation. *J. Climate,* **20,** 4316–4340.

Wang, S.-Y., R. R. Gillies, E. S. Takle, and W. J. Gutowski Jr., 2009: Evaluation of precipitation in the Intermountain Region as simulated by the NARCCAP regional climate models. *Geophys. Res. Lett.,* **36,** L11704, doi:10.1029/2009GL037930.

Wood, A. W., L. R. Leung, V. Sridhar, and D. P. Lettenmaier, 2004: Hydrologic implications of dynamical and statistical approaches to downscaling climate model outputs. *Climatic Change,* **62,** 189–216.

Yin, J. H., 2005: A consistent poleward shift of the storm tracks in simulations of 21st century climate. *Geophys. Res. Lett.,* **32,** L18701, doi:10.1029/2005GL023684.

Zhu, C., D. P. Lettenmaier, and T. Cavazos, 2005: Role of antecedent land surface conditions on monsoon rainfall variability. *J. Climate,* **18,** 2824–2841.

——, T. Cavazos, and D. P. Lettenmaier, 2007: Role of antecedent land surface conditions in warm season precipitation over northwestern Mexico. *J. Climate,* **20,** 1774–1791.